Supplementary Data

Supplementary Materials and Methods

Construction of STAT3 mammalian expression plasmids and site-directed mutagenesis

Mouse STAT3 cDNA in pBluescript (pBS-mSTAT3) was purchased from ThemoFisher Scientific (Open Biosystem, Huntsville, AL). Using this plasmid as a template, *Nhe*I and *Eco*RI cleavage sites for mammalian expression plasmid construction were created with polymerase chain reaction (PCR) using the following flanking primers: STAT3 (Flnk-forward: 5′-ACC CCG CTA GCC AGC AGG ATG G-3′ and Flnk-reverse: 5′-TCA GCG AAT TCC ATG GGG GAG GTA-3′). Following the amplification, the resulting PCR product containing wild-type cDNA (*Nhe*I-*wt*STAT3-*Eco*RI) was ligated into pcDNA3-Myc-His plasmid (Invitrogen, Carlsbad, CA) *via Nhe*I/*Eco*RI-sites. To identify the target Cys residue(s) for S-nitrosylation, *wt*STAT3 gene (aa 1-769) was sequentially deleted; the deletion mutants were designated as *f1* (aa 1-580) and *f2* (aa 1-314) (Fig. 5A-ii). The f1 or f2 deletion mutant expression plasmid were constructed by PCR amplification of pBS-mSTAT3 with the following primer sets: f1 (forward: 5′-ACC CCG CTA GCC AGC AGG ATG G-3′ and reverse: 5′-TAC CCG AAT TCC CAA AGG GCC AAG-3′) and f2 (forward: 5′-ACC CCG CTA GCC AGC AGG ATG G-3′ and reverse: 5′-TTC ATG AAT TCT CTG AAC AGC TCC-3′). After the amplification, the resulting PCR products were ligated into pcDNA3-Myc-His plasmid (Invitrogen) *via Nhe*I/*Eco*RI-sites.

Site-directed mutagenesis of Cys via *overlap extension*

STAT3 contains 14 Cys residues (Fig. 6A-i). For replacement of each Cys residue with Ala, 14 sets of internal primers were designed as listed in Supplementary Table S1 and used for generation 2 PCR products that contain overlap extension. Each PCR reaction was performed by Pfu DNA polymerase (Invitrogen) with one of flanking primers (Flnk-forward or Flnk-reverse) that hybridizes at one end of template (*Nhe*I-*wt*STAT3-*Eco*RI) and one internal primer that hybridizes at the site of mutation. Following the amplification and purification of PCR products, the two fragments carrying sequence overlaps were fused by incubation with Tag DNA polymerase (Invitrogen) and amplified by the addition of flanking primer set. The resulted PCR product containing mutant cDNA (*Nhe*I-*mt*STAT3-*Eco*RI) was ligated into pcDNA3-Myc-His plasmid (Invitrogen) *via Nhe*I/*Eco*RI-sites. To identify the Cys→Ala mutation, we performed DNA sequence analysis of each plasmid.

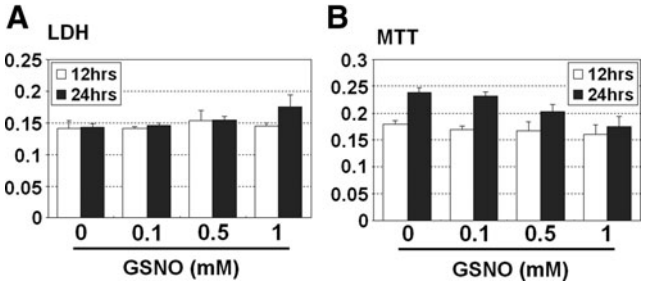

SUPPLEMENTARY FIG. S1. Effect of GSNO on cell toxicity. To examine the possible cell toxicity following GSNO treatment, BV2 cells were treated with GSNO (0, 0.1, 0.5, and 1 m*M*) for 12 and 24 h and cell toxicity and viability were analyzed by lactate dehydrogenase (LDH) activity assay **(A)** and MTT assay **(B)**, respectively. LDH assay was performed by using the LDH assay kit from Roche (Indianapolis, IN). MTT assay was performed as described under the Materials and Methods section. The results from LDH assay document that GSNO (≤1 m*M*) did not produce any significant cell toxicity in BV2 cells up to 24 h. The MTT assay show that GSNO has no effect on cell viability at 12 h after the treatment. At 24 h, BV2 cells shows increased MTT reduction to formazan compared to the value measured at 12 h due to increased cell number. The increased MTT reduction to formazan was inhibited by treatment with GSNO in a dose-dependent manner. Along with the data shown in Figure 3B-ii describing the inhibitory effect of GSNO in BV2 cell proliferation, these data also suggest that GSNO inhibits cell proliferation without inducing cytotoxicity. GSNO, S-nitrosoglutathione; MTT, 3-(4,5-dimethylthiazol-2-yl)-2,5-diphenyltetrazolium bromide.

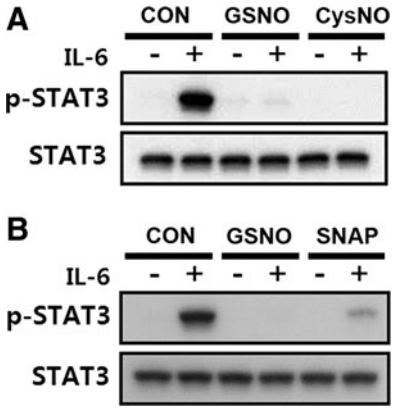

SUPPLEMENTARY FIG. S2. Effect of S-nitroso-N-acetylpenicillamine (SNAP) on STAT3 Y705 phosphorylation in BV2 cells. The effect of GSNO (500 μM/2 h), S-nitrosocysteine (CysNO; 500 μM/2 h) **(A),** and SNAP (500 μM/2 h) **(B)** on IL-6-induced (30 ng/ml) STAT3 (Y705) phosphorylation was analyzed by Western analysis. These data indicate that SNAP, a S-nitrosyl donor, inhibits IL-6-induced STAT3 phosphorylation similar to the effect of GSNO. IL-6, interleukin-6; STAT3, signal transducer and activator of transcription 3.

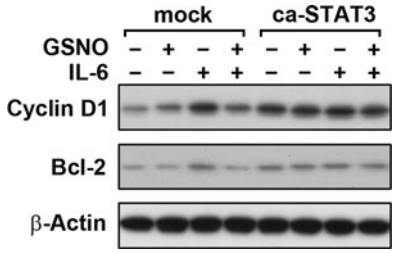

SUPPLEMENTARY FIG. S3. Role of STAT3 in GSNO-mediated regulation of Cyclin D1 and Bcl-2. To access whether STAT3 in involved in GSNO-induced reduction in Cyclin D1 and Bcl-2 expression in Figure 2B, CHO cells were transfected with mock control (pcDNA3 only) or constitutive active STAT3 (ca-STAT3) mutant and the effects of GSNO treatment on IL-6 induced expression of Cyclin D1 and Bcl-2 were analyzed by Western analysis. The cells were treated with GSNO (500 μM) for 2 h before IL-6 treatment. Eighteen hours after IL-6 treatment, the cells were harvested for Western analysis. In this study, we observed that CHO cells also expressed increased protein levels of cyclin D1 and Bcl-2 following IL-6 treatment and GSNO treatment decreased IL-6-induced increases of these proteins. Transfection of CHO cells with constitutive active STAT3 (ca-STAT3) also increased expressions of cyclin D1 and Bcl-2. However, GSNO treatment was not able to decrease the ca-STAT3-induced increases in protein levels of cyclin D1 and Bcl-2. These data indicate that GSNO may regulate the expression of cyclin D1 and Bcl-2 *via* STAT3-dependent pathway. CHO, Chinese hamster ovary.

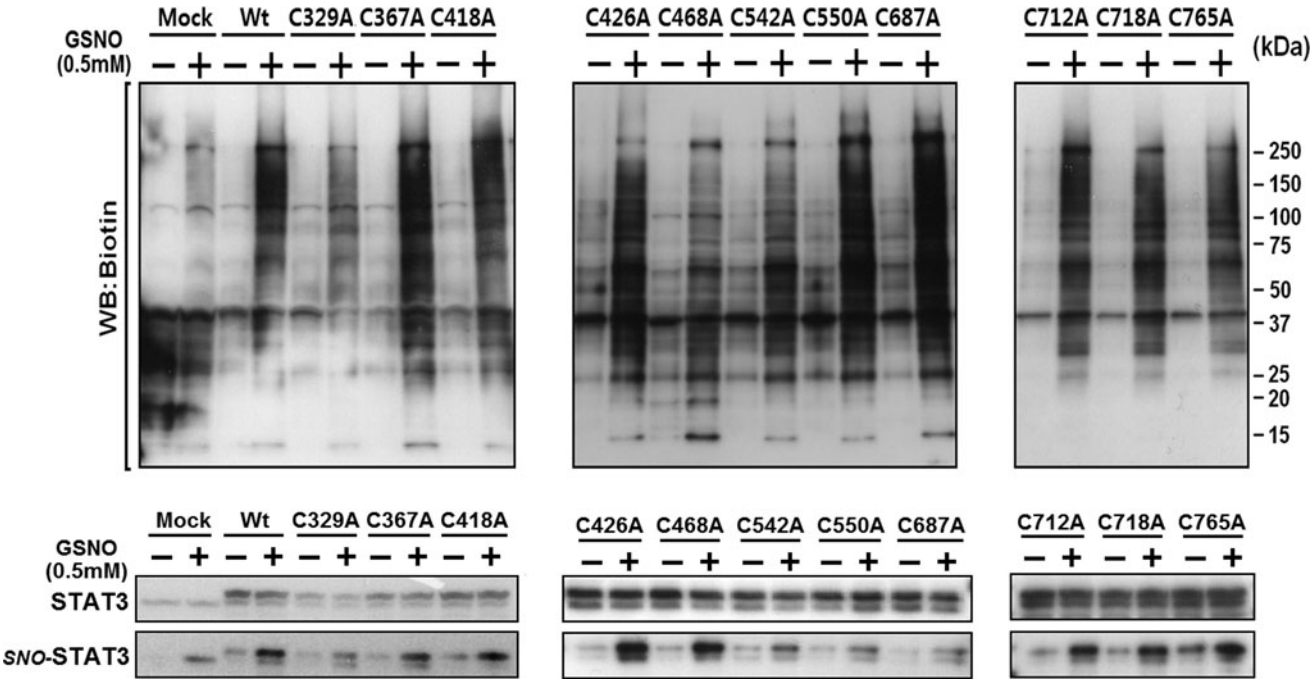

SUPPLEMENTARY FIG. S4. Effect of point mutation of each Cys residue to Ala on STAT3 S-nitrosylation. As described under the Materials and Methods section, other Cys residues, in addition to Cys 108, 251, 259, were replaced with Ala by point mutation and the effect of GSNO on the nitrosylation of recombinant STAT3 was analyzed by biotin switch assay. In these experiments, we confirm that none of Cys other than Cys259 is involved in GSNO-mediated S-nitrosylation of STAT3.

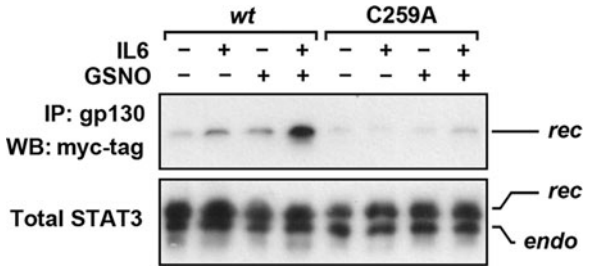

SUPPLEMENTARY FIG. S5. Effect of GSNO on STAT3 recruitment to gp130. To assess whether S-nitrosylation of Cys^{259} inhibits STAT3 Tyr^{705} phosphorylation through inhibiting STAT3/gp130 interaction by altering the function and structure of coiled-coil (CC) domain, CHO cells were transiently transfected with wild-type (*wt*) STAT3 or C259A mutant STAT3 expressing vectors. Following the treatment of cells with GSNO (300 μM) for 2 h and then IL-6 (30 ng/mL) for 30 min, the cells were lysed with RIPA buffer and subjected to immunoprecipitation using antibody specific to gp130. The levels of co-precipitated recombinant *wt*STAT3 or C259A mutant STAT3 were analyzed by Western analysis using antibody specific to myc-tag. Western analysis of total STAT3 from whole cell lysates were used as standard for expression levels of recombinant (*rec*) or endogenous (*endo*) STAT3s. The figure shows that the treatment of CHO cells expressing recombinant *wt*STAT3 with GSNO or IL-6 slightly increased the recruitment of STAT3 to gp130. In addition, the recruitment of recombinant *wt*STAT3 to gp130 was greatly enhanced when the cells were treated with GSNO and IL-6 simultaneously. In the cells expressing C259A mutant STAT3, however, neither GSNO, IL-6, nor GSNO and IL-6 combination increased STAT3 recruitment to gp130. Taken together with the data reported in Figure 4, these data suggest that GSNO-mediated S-nitrosylation of Cys^{259} in STAT3 appears to inhibit JAK2 accessibility to STAT3 in gp130 receptor complex and thus inhibits Tyr^{705} phosphorylation. Consequently, GSNO appears to inhibit STAT3 release from gp130 complex. JAK2, Janus-activated kinase 2.

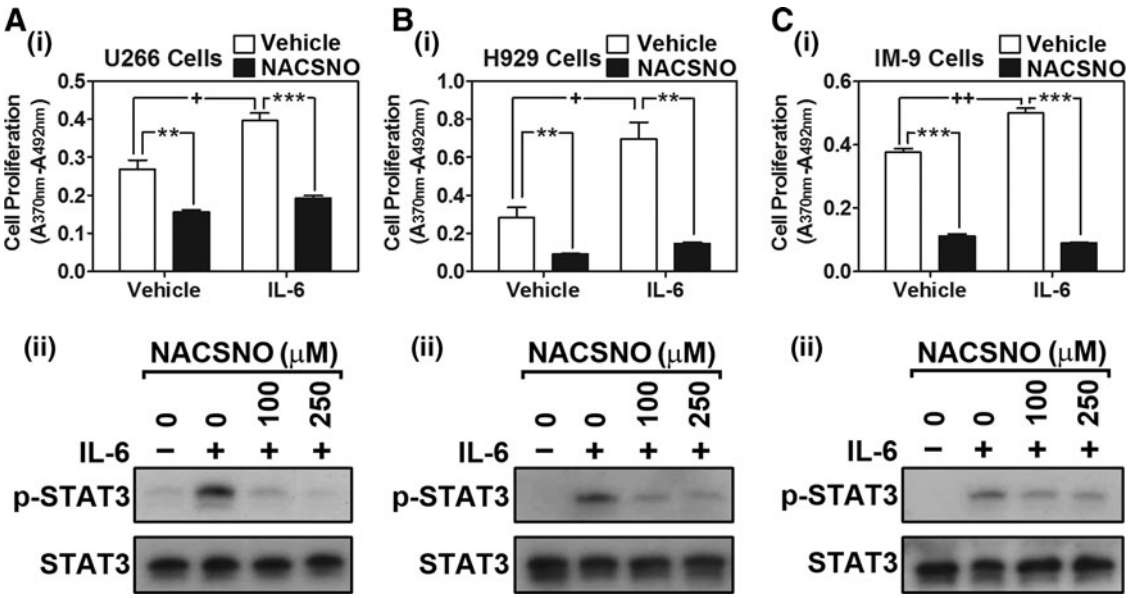

SUPPLEMENTARY FIG. S6. Effect of NACSNO on the proliferation of cancer cell lines. To assess whether NACSNO treatment inhibits cancer cell proliferation and STAT3 activation, BrdU incorporation assay **(i)** and Western analysis for phospho- and pan-STAT3 **(ii)** were performed using human multiple myeloma cell lines including U266 **(A)**, H929 **(B)**, and IM-9 **(C)**. Supplementary Figure S2A-i, B-i, and C-i show that NACSNO treatment (2 h before and 12 h after 20 ng/ml IL-6 treatment; 200 μM each) inhibits proliferation of all three cell lines under basal and IL-6-stimulated conditions. Supplementary Figure S2A-ii, B-ii, and C-ii shows that NACSNO treatment (100 and 250 μM for 2 h) inhibits IL-6-induced (20 ng/ml for 0.5 h) STAT3 phosphorylation without altering total STAT3 protein levels. These data suggest S-nitrosylation mechanism as potential antitumor cell signaling pathway. BrdU, 5-bromo-2′-deoxyuridine; NACSNO, S-nitroso-N-acetyl cysteine.

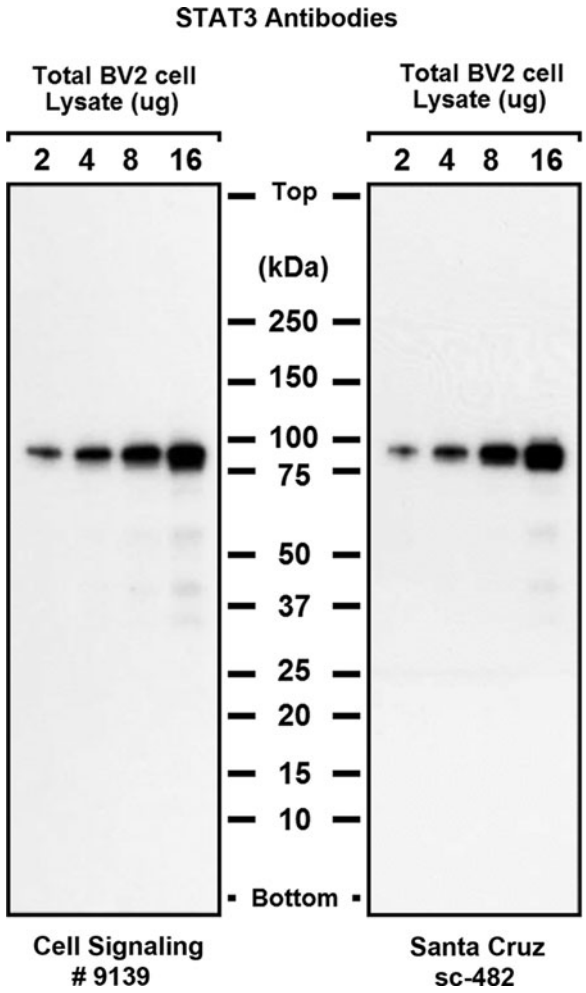

SUPPLEMENTARY FIG. S7. Specificities of antibodies against STAT3 for ELISA assay. The specificity of STAT3 antibodies was tested by Western analysis using the control cell lysates of BV2 cells. Both antibodies (Cell Signaling; #9139 and Santa Cruz Biotechnology; #SC-482) showed almost identical pattern of blots; one major band at 88 kDa (between 75 and 100 kDa) and three to four minor bands with lower molecular weight that may be proteolytic fragments of STAT3. The band localized at 88 kDa (STAT3) were more than 93% of total intensities, indicating the specific interaction of these antibodies with STAT3. ELISA, enzyme-linked immunosorbent assay.

Supplementary Table S1. Internal Primer Sequences for Polymerase Chain Reaction-Based Site-Directed Mutagenesis *via* Overlap Extension for Replacement of Cysteine Residues with Alanine

Cysteine positions	*Directions*	*Primer sequences*
C108A	F	5′-GAT CGT GGC CCG AGC CCT GTG-3′
	R	5′-CAC AGG GCT CGG GCC ACG ATC-3′
C251A	F	5′-GCA GAT CGC GGC CAT CGG AG-3′
	R	5′-CTC CGA TGG CCG CGA TCT GC-3′
C259A	F	5′-CAA CAT CGC CCT GGA CCG TC-3′
	R	5′-GAC GGT CCA GGG CGA TGT TG-3′
C328A	F	5′-GGA GCG GCA GCC CGC CAT GC-3′
	R	5′-GCA TGG CGG GCT GCC GCT CC-3′
C367A	F	5′-GTG GCC ATT GAT AAA GAC TC-3′
	R	5′-GAG TCT TTA TCA ATG GCC AC-3′
C418A	F	5′-GAG CAG AGA GCT GGG AAT G-3′
	R	5′-CAT TCC CAG CTC TCT GCT C-3′
C426A	F	5′-GCC GTG CCA ATG CTG ATG C-3′
	R	5′-GCA TCA GCA TTG GCA CGG C-3′
C468A	F	5′-CGC TCA GAT GCC AAA TGC T-3′
	R	5′-AGC ATT TGG CAT CTG AGC G-3′
C542A	F	5′-GAT CAC ATG GGC TAA ATT CGC C-3′
	R	5′-GGC GAA TTT AGC CCA TGT GAT C-3′
C550A	F	5′-TCG CCA AAG AAA ACA TGG CTG G-3′
	R	5′-CCA GCC ATG TTT TCT TTG GCG A-3′
C687A	F	5′-AAG TAC GCT AGG CCC GAG A-3′
	R	5′-TCT CGG GCC TAG CGT ACT T-3′
C712A	F	5′-ACC AAG TTC ATC GCT GTG AC-3′
	R	5′-GTC ACA GCG ATG AAC TTG GT-3′
C718A	F	5′-CAA CGA CCG CCA GCA ATA C-3′
	R	5′-GTA TTG CTG GCG GTC GTT G-3′
C765A	F	5′-CTG ACC TCG GAG GCT GCT A-3′
	R	5′-TAG CAG CCT CCG AGG TCA G-3′